

Learning to predict synchronization of coupled oscillators on heterogeneous graphs

Hardeep Bassi,^{1, a)} Richard Yim,^{2, a)} Rohith Kodukula,² Joshua Vendrow,^{2, b)} Cherlin Zhu,³ and Hanbaek Lyu^{2, c)}

¹⁾*Department of Mathematics, University of California, Berkeley, CA 94720, USA*

²⁾*Department of Mathematics, University of California, Los Angeles, CA 90095, USA*

³⁾*Department of Applied Mathematics and Statistics, Johns Hopkins University, Baltimore, MD 21218, USA*

Suppose we are given a system of coupled oscillators on an arbitrary graph along with the trajectory of the system during some period. Can we predict whether the system will eventually synchronize? This is an important but analytically intractable question especially when the structure of the underlying graph is highly varied. In this work, we take an entirely different approach that we call “learning to predict synchronization” (L2PSync), by viewing it as a classification problem for sets of graphs paired with initial dynamics into two classes: ‘synchronizing’ or ‘non-synchronizing’. Our conclusion is that, once trained on large enough datasets of synchronizing and non-synchronizing dynamics on heterogeneous sets of graphs, a number of binary classification algorithms can successfully predict the future of an unknown system with surprising accuracy. We also propose an “ensemble prediction” algorithm that scales up our method to large graphs by training on dynamics observed from multiple random subgraphs. We find that in many instances, the first few iterations of the dynamics are far more important than the static features of the graphs. We demonstrate our method on three models of continuous and discrete coupled oscillators — The Kuramoto model, the Firefly Cellular Automata, and the Greenberg-Hastings model.

I. INTRODUCTION

A. Overview

Many important phenomena that we would like to understand – formation of public opinion, trending topics on social networks, movement of stock markets, development of cancer cells, outbreak of epidemics, and collective computation in distributed systems – are closely related to predicting large-scale behaviors in networks of locally interacting dynamic agents. Perhaps the most widely studied and mathematically intractable of such collective behavior is the *synchronization* of coupled oscillators (e.g., blinking fireflies, circadian pacemakers, BZ chemical oscillators), and has been an important subject of research in mathematics and various areas of science for decades^{1,42}. Moreover, it is closely related to the *clock synchronization* problem, which is essential in establishing shared notions of time in distribution systems, and has enjoyed fruitful applications in many areas including wildfire monitoring, electric power networks, robotic vehicle networks, large-scale information fusion, and wireless sensor networks^{9,35,39}.

In this paper, we are concerned with the fundamental problem of *predicting whether a given system of coupled oscillators will eventually synchronize*. The answer depends on

roughly three types of information: 1) model parameters, 2) initial configuration, and 3) graph structure. While a number of sufficient conditions on model parameters (e.g., large coupling strength) or on initial configuration (e.g., phase concentration into open half-circle) for synchronization are known, our understanding of the influence of graph structure on long-term dynamics is still relatively restricted. This is mainly due to the fact that obtaining an analytic or asymptotic solution to the prediction problem in general appears to be out of reach, especially when the underlying graphs are heterogeneous and the initial phases are not concentrated. In this work, ‘heterogeneous graphs’ refers to sets of non-isomorphic simple graphs, where there is one type of node and edge but the connection topology is diverse. Since the global behavior of coupled oscillators is built on non-linear local interactions, as the number of nodes increase and the graphs become more heterogeneous, the behavior of the system becomes rapidly unpredictable. To provide a sense of the complexity of the problem, note that there are more than 10^9 non-isomorphic connected simple graphs with 11 nodes³³.

But is it really that unpredictable? In this work, we propose a radically different approach to this problem that we call *Learning To Predict Synchronization* (L2PSync), where we view it as a classification problem for graphs, paired with initial dynamics, into one of two classes of ‘synchronizing’ and ‘non-synchronizing’ oscillators. We empirically show that once trained on large enough datasets of synchronizing and non-synchronizing dynamics on heterogeneous graphs, a number of binary classification algorithms can in fact successfully predict the future of an unknown system with surprising accuracy. Moreover, we find that in many instances the first few iterations of dynamics are far more important than the static features of a graph. We demonstrate our methods on

^{a)}Co-first author

^{b)}<http://www.joshvendrow.com>

^{c)}<http://www.hanbaeklyu.com>; Supported by NSF DMS-2010035

The codes for the main algorithm and simulations are provided in <https://github.com/richpaulyim/L2PSync>

three models of continuous and discrete coupled oscillators — the Kuramoto model (KM)¹, the Firefly Cellular Automata (FCA)²⁷, and the Greenberg-Hastings model (GHM)¹⁸.

The pipeline of our approach is as follows. Namely, 1) fix a model for coupled oscillators; 2) generate a *dynamics dataset* of non-isomorphic graphs with equal parts non-synchronizing and synchronizing examples for a large number of synchronizing and non-synchronizing examples, with even split between classes on non-isomorphic graphs; 3) train a selected binary classification algorithm on the dynamics dataset to classify each example (graph paired with initial dynamics) into one of two classes, ‘synchronizing’ or ‘non-synchronizing’; 4) finally, validate the accuracy of the trained algorithms on fresh examples by comparing the predicted behavior of the true long-term dynamics. We use the following classification algorithms: Random Forest (RF)⁴ Gradient Boosting (GB)¹⁵, Feed-forward Neural Networks (FFNN)³, and our own adaptation of Long-term Recurrent Convolutional Networks (LRCN)⁸ which we call the *GraphLRCN*.

As a baseline for our approach, we use a variant of the well-known “concentration principle” in the literature of coupled oscillators. Namely, regardless of the details of graph structure and model, synchronization is guaranteed if the initial phases of the oscillators are concentrated in a small arc of the phase space (see Subsection III A). Regardless of the three models of coupled oscillators and selected binary classification algorithm, we find that our method on average shows at least a 30% improvement in prediction performance compared to this concentration-prediction baseline for dynamics on 30 node graphs.

In order to reduce the computational cost of applying our pipeline to larger graphs, we also propose an “ensemble prediction” algorithm (Algorithm 1) that scales up our method to large graphs by training on dynamics observed from multiple random subgraphs. Namely, if we are to learn dynamics on connected N -node graphs, then we take a sample of relatively small induced subgraphs on n nodes ($n \ll N$), along with the induced dynamics, and train a binary classification algorithm on the dynamics observed from those sampled subgraphs. We then aggregate the predictions from each subgraph (e.g., using majority vote) to get a prediction for the full dynamics. Using this method, we achieve an area-under-curve (AUC) score of about 0.85 for predicting the FCA dynamics on 600 node graphs by only using two 30-node subgraphs.

From the robustness of our prediction accuracy with respect to both the continuous and discrete models as well as the binary classification algorithm of choice, we believe that our method of “learning to predict synchronization” can be generalized to “learning to predict complex systems”.

B. Problem statement and our approach

A graph $G = (V, E)$ consists of sets V of nodes and E of edges. Let Ω denote the *phase space* of each node, which may be taken to be the circle $\mathbb{R}/2\pi\mathbb{Z}$ for continuous-state oscillators or the color wheel $\mathbb{Z}/\kappa\mathbb{Z}$, $\kappa \in \mathbb{N}$ for discrete-state oscillators. We call a map $X : V \rightarrow \Omega$ a *phase configuration*, and

say it is *synchronized* if it takes a constant value across nodes (i.e., $X(v) = \text{Const.}$ for all $v \in V$). A *coupling* is a function \mathcal{F} that maps each pair (G, X_0) of graph and initial configuration $X_0 : V \rightarrow \Omega$ deterministically to a *trajectory* $(X_t)_{t \geq 0}$ of phase configurations $X_t : V \rightarrow \Omega$. For instance, \mathcal{F} could be the time evolution rule for the KM, FCA, or GHM. The main problem we investigate in this work is stated below:

Problem I.1 (Synchronization Prediction) Fix parameters $n \in \mathbb{N}$, $r > 0$, and coupling \mathcal{F} . Given a connected graph G and trajectory $(X_t)_{0 \leq t \leq r}$, predict the following indicator

$$\mathbf{1}(X_t \text{ is eventually synchronized}). \quad (1)$$

See Figure 4 for illustration.

C. Related works

There are a number of recent works on learning features of dynamical systems from fixed graphs. Itabashi et al.²² used topological data analysis (TDA) to map trajectories of Kuramoto oscillator phases onto a manifold, and extracted time-varying topological features of the dynamics. One of their goals was to learn characterizations of multi-cluster synchronized dynamics at an early stage where oscillators are all-to-all connected, but permitted to form a few clusters. Thiem et al.⁴⁴ used neural networks (NN) to learn coarse-grained dynamics of Kuramoto oscillators and recovered the classical order parameter. Biccari et al.² used gradient descent (GD) and the random batch method (RBM) to learn control parameters to enhance synchronization of Kuramoto oscillators. Slightly less related work is Hefny et al.¹⁹, where the authors used hidden Markov models, lasso regression and spectral algorithms for learning lower-dimensional state representations of dynamical systems, and applied their method on a knowledge tracing model for a dataset of students’ responses to a survey.

References	# nodes	# graphs	# configs.	model	ML
Itabashi et al. ²²	128-256	1	100	KM	TDA
Thiem et al. ⁴⁴	1500-8000	1	2000	KM	NN
Biccari et al. ²	10-1000	1	1	KM	GD,RBM
This work	15-600	64K-200K	1	KM, FCA, GHM	RF, GB, FFNN, LRCN

TABLE I. Comparison of settings in related works on learning coupled oscillator dynamics using machine learning methods. Recent works^{2,22,44} focus on learning features of dynamics on fixed graphs. In contrast, we aim to learn how an underlying graph structure influences long-term dynamics. The column for ‘# configs.’ refers to the number of distinct initial phase configurations considered for each graph in training.

It is important to note that the focus of the aforementioned works is to learn features of dynamics on a fixed graph. For this purpose, it is natural to fix an underlying graph (mostly all-to-all) and simulate trajectories from multiple initial configurations and learn features of the generated dynamics. In contrast, our goal is to learn how the underlying structure of

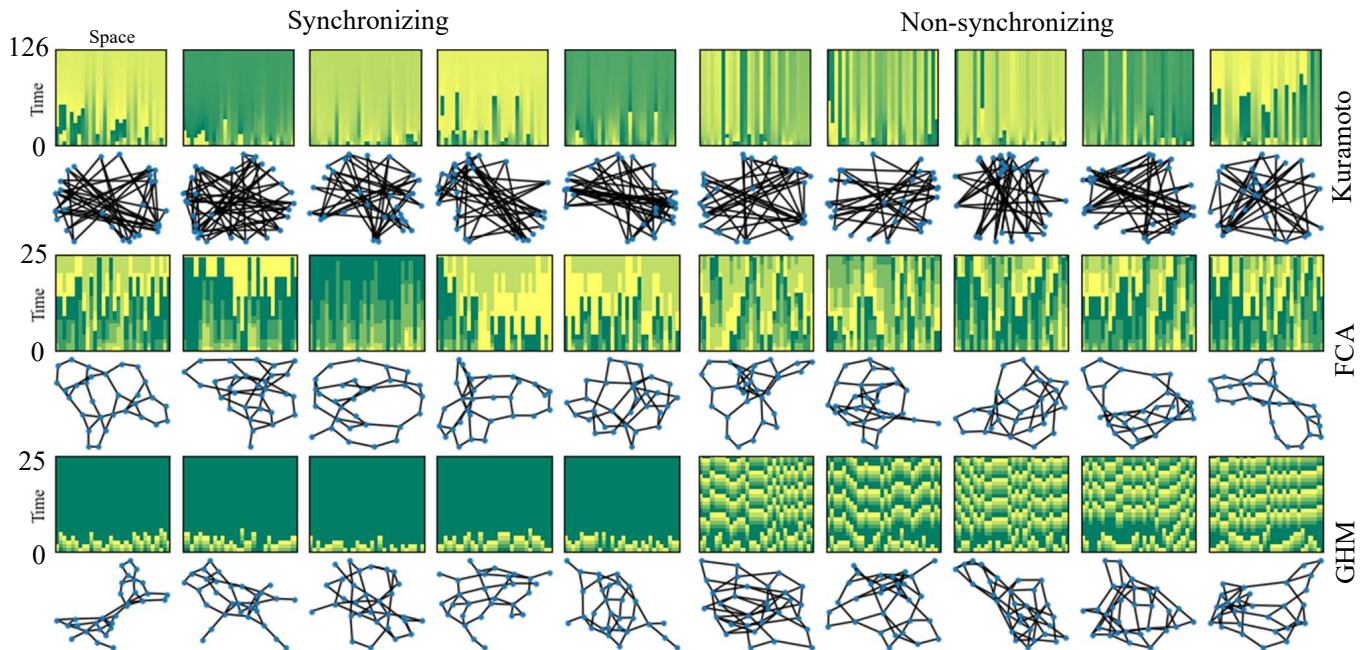


FIG. 1. Sample points in the 30-node dynamics dataset for synchronization prediction. The heat maps show phase dynamics on graphs beneath them, where colors represent phases and time is measured by iterations from bottom-to-top (e.g. $t = 0$ to $t = 25$). Each example is labeled as ‘synchronizing’ if it synchronizes at iteration 1758 for the Kuramoto model (70 for FCA and GHM) and ‘non-synchronizing’ otherwise. Synchronizing examples have mostly uniform color in the top row. For training, only a portion of dynamics is used so that the algorithms rarely see a fully synchronized example (see Figure 4).

a graph influences long-term dynamics. Hence, in our setting we generate a large number (80K-200K) of non-isomorphic graphs (15-600 nodes) with a single initial configuration, and train a machine learning algorithm so that it can correctly classify whether a given graph paired with an initial configuration will eventually synchronize. Random Forest (RF)⁴, Gradient Boosting (GB)¹⁵, Feed-forward Neural Networks (FFNN)³ and Long-term Recurrent Convolutional Networks (LRCN)⁸ are the machine learning models that were applied in our problem. Also, while the works^{2,22,44} only consider the Kuramoto model (KM) and algorithms are trained on graphs with fixed size, we additionally consider two discrete models: Firefly Cellular Automata (FCA)²⁷ and the Greenberg-Hastings Model (GHM)¹⁸ and also develop an algorithm where the size of the graph need not be fixed.

We remark that there are a number of cases where rigorous results are available for the question of predicting the long term behavior of a coupled oscillators on a graph G and initial configuration X_0 . For instance, the $\kappa = 3$ instances of GHM and another related model called Cyclic Cellular Automata (CCA)¹¹ have been completely solved¹⁷. Namely, given the pair (G, X_0) , the trajectory X_t synchronizes eventually if and only if the discrete vector field on the edges of G induced from X_0 is conservative (see¹⁷ for details). Additionally, the behavior of FCA on finite trees is also well-known: given a finite tree T and $\kappa \in \{3, 4, 5, 6\}$, every κ -color initial configuration on T synchronizes eventually under κ -color FCA if and only if κ is strictly less than the maximum degree of T ; for $\kappa \geq 7$, this phenomenon does not always hold^{27,28}. Fur-

thermore, there is a number of works on the clustering behavior of these models on the infinite one-dimensional lattice, \mathbb{Z} (FCA^{30,31}, CCA^{12-14,30} and GHM^{10,30}).

II. BACKGROUNDS

A. Three models for coupled oscillators

The *Kuramoto model* (KM) is one of the most well-studied models for coupled oscillators with continuous states^{1,25,26,42}. Namely, fix a graph $G = (V, E)$ and the continuous state space $\Omega = \mathbb{R}/2\pi\mathbb{Z}$. A given initial phase configuration $X_0 : V \rightarrow \Omega$ evolves via the following systems of ordinary differential equations

$$\frac{d}{dt}X_t(v) = \omega_v + \sum_{u \in N(v)} K \sin(X_t(u) - X_t(v)), \quad (2)$$

for all nodes $v \in V$, where $N(v)$ denotes the set of neighbors of v in G , K denotes the *coupling strength*, and ω_v denotes the *intrinsic frequency* of v . Since we are interested in the dichotomy between synchronization and non-synchronization, we will be assuming identical intrinsic frequencies, which can be assumed to be zero without loss of generality by using a rotating frame. Note that synchronization is an *absorbing state* under this assumption, that is, X_t is synchronized for all $t \geq s$ if X_s is synchronized. In order to simulate KM, we use the

following discretization

$$X_{t+h}(v) - X_t(v) = h \left(\sum_{u \in N(v)} K \sin(X_t(u) - X_t(v)) \right), \quad (3)$$

with step size $h = 0.05$. Accordingly, an ‘iteration’ for KM is a single application of the difference equation (3). After a change of time scale, we write X_k for the configuration obtained after k iterations.

We also consider two discrete models for coupled oscillators. Let $\Omega = \mathbb{N}/\kappa\mathbb{Z}$ be the κ -state color wheel for some integer $\kappa \geq 3$. The κ -color *Firefly Cellular Automata* (FCA) is a discrete-state discrete-time model for inhibitory Pulse Coupled Oscillators (PCOs) introduced by Lyu²⁷. The intuition is that we view each node as an identical oscillator (firefly) of κ -states, which *blinks* whenever it returns to a designated *blinking color* $b(\kappa) = \lfloor \frac{\kappa-1}{2} \rfloor$; nodes with post-blinking color $c \in (b(\kappa), \kappa - 1]$ in contact with at least one blinking neighbor do not advance, as if their phase update is being inhibited by the blinking neighbors, and otherwise advance to the next color (see Figure 2). More precisely, the coupling for FCA is defined as the following difference equation

$$X_{t+1}(v) - X_t(v) = \begin{cases} 0 & \text{if } X_t(v) > b(\kappa) \text{ and } X_t(u) = b(\kappa) \text{ for some } u \in N(v) \\ 1 & \text{otherwise.} \end{cases} \quad (4)$$

For visualization purposes, it is convenient to consider the equivalent dynamics of ‘centered colorings’ $\bar{X}_t := X_t - t \pmod{\kappa}$, so that if X_t synchronizes, then \bar{X}_t converges to a constant function. In fact, FCA dynamics are displayed in this way in Figures 1 and 4.

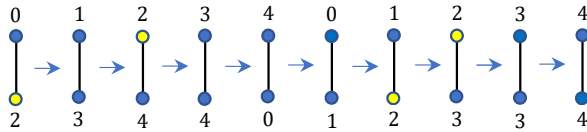


FIG. 2. An example of 5-color FCA dynamics on two connected nodes. $b(5) = 2$ is the blinking color shown in yellow.

On the other hand, the *Greenberg-Hastings model* (GHM) is a discrete model for neural networks¹⁸ introduced in 1987 by Greenberg and Hastings, where nodes of color 0 and 1 are called ‘rested’ and ‘excited’, respectively, and of any other color called ‘refractory’. As in biological neural networks, rested neurons gets excited by neighboring excited nodes, and once excited, it has to spend some time in rested states to come back to the rested state again. More precisely, the coupling for GHM is defined as

$$X_{t+1}(v) = \begin{cases} 0 & \text{if } X_t(v) = 0 \text{ and } X_t(u) \neq 1 \text{ for all } u \in N(v) \\ 1 & \text{if } X_t(v) = 0 \text{ and } X_t(u) = 1 \text{ for some } u \in N(v) \\ X_t(v) + 1 & \text{otherwise.} \end{cases} \quad (5)$$

For GHM, note that X_s is synchronized if and only if $X_t \equiv 0$ for all $t \geq s + \kappa$.

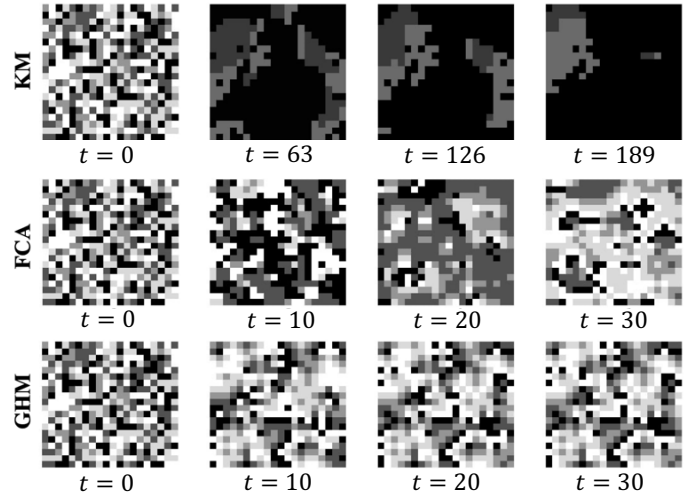


FIG. 3. Simulation of KM, FCA, and GHM on the same underlying graph and initial configuration. The graph is generated by adding 80 edges uniformly at random into 20×20 square lattice. Each square heap map represents a phase configuration X_t at the corresponding iteration t shown below.

In all experiments in this paper, we consider $\kappa = 5$ instances of FCA and GHM. From here and hereafter, by FCA and GHM we mean the 5-color FCA and 5-color GHM, respectively.

While all three models tend to synchronize locally their global behavior on the same graph and initial configuration evolve quite differently, as seen in Figure 3. There, we simulate each system on the same graph, a 20×20 lattice with an additional 80 edges added uniformly at random. A single initial phase concentration X_0 is chosen by assigning each node with a uniformly randomly chosen state from $\{0, 1, 2, 3, 4\}$. This initial configuration is evolved through three different models: FCA, GHM and KM.

This suggests that it is not feasible to predict synchronization for all three dynamics in the same way. Furthermore, the inclusion of random edges to the square lattice may disrupt some well-known behavior (e.g., spiral waves for coupled oscillators in 2D lattice³²) and result in unpredictable dynamics, analytically so. Hence, predicting synchronization on fully heterogeneous sets of graphs (see Figures 1 and 4) is a difficult task since keeping track of local interactions of oscillators is challenging to do when the overall structures of graphs within the heterogeneous set correspondingly have highly irregular and diverse couplings.

III. METHODS

A. The concentration principle for synchronization and baseline predictor

In the literature of coupled oscillators, there is a fundamental observation that concentration (e.g., into an open half-circle) of initial phase of the oscillators leads to synchronization for a wide variety of models on arbitrary connected graphs (see, e.g.,²⁹ (Lem 5.5)). This is stated in Lemma III.1

for KM and FCA and we call it as the ‘‘concentration principle’’. This principle has been used pervasively in the literature of clock synchronization^{23,37,38,41} and also in multi-agent consensus problems^{5,34,40}.

Lemma III.1 (Concentration principle) *Let G be an arbitrary connected graph. For Kuramoto model (2) with identical intrinsic frequency and for FCA (4), any initial phase configuration on G synchronizes if all phases are confined in an open half-circle in the phase space Ω .*

In the above lemma, the ‘open half-circle’ refers to any arc of length $< \pi$ for the continuous state space $\Omega = \mathbb{R}/2\pi\mathbb{Z}$ and any interval of $< \kappa/2$ consecutive integers (mod κ) for the discrete state space $\Omega = \mathbb{Z}/\kappa\mathbb{Z}$. This is a standard fact known to the literature and it follows from the fact that the couplings in the statement monotonically contract given any initial phase configuration under the half-circle condition toward synchronization. An important corollary is the following:

Corollary III.2 *Let G be an arbitrary connected graph. For Kuramoto model (2) with identical intrinsic frequency and for FCA (4), if all states used in the time- t configuration X_t are confined in an open half-circle, then the trajectory on G eventually synchronizes.*

It is not hard to see that Corollary III.2 does not hold for GHM. We define

$$X_r \text{ is concentrated} \quad (6)$$

$$\stackrel{\text{def}}{\iff} \left\{ \begin{array}{l} X_r \text{ is confined in an} \\ \text{open half-circle of } \Omega \end{array} \right\} \text{ for KM and FCA}$$

$$\left\{ \begin{array}{l} X_r \text{ is synchronized} \end{array} \right\} \text{ for GHM.}$$

We now introduce the following baseline synchronization predictor: Given $(X_t)_{0 \leq t \leq r}$ and $T > r$,

Baseline predictor: Predict synchronization of X_T if X_r is concentrated; Otherwise, flip a fair coin.

Notice that by Corollary III.2, the baseline predictor never predicts synchronization incorrectly if X_r is concentrated. For non-concentrated cases, the baseline does not assume any knowledge and gives a completely uninformed prediction. Quantitatively, suppose we use this baseline predictor for a dataset where α proportion of samples are synchronizing where we use the first r iterations of dynamics for each sample. Let $x = x(r)$ denote the proportion of synchronizing samples among all synchronizing samples that concentrate by iteration r . Then the baseline predictor’s accuracy is given by $0.5 + x\alpha/2$, where the second term can be regarded as the gain obtained by using Corollary III.2 layered onto the uninformed decision.

B. Generating the dynamics datasets

We generate a total of nine datasets described in Tables III and IV for studying the synchronization prediction problem

(Problem I.1). Data points in each dataset consist of three statistics computed for a pair (G, X_0) of an underlying graph, $G = (V, E)$, and initial configuration, $X_0 : V \rightarrow \Omega$: 1) first r iterations of dynamics $(X_t)_{0 \leq t \leq r}$ (using either KM, FCA, or GHM), 2) features of G and X_0 , and 3) the label that indicates whether X_T is concentrated or not (see Table II). We say a data point is ‘synchronizing’ if the label is 1, and ‘non-synchronizing’ otherwise. Every dataset we generate contains an equal number of synchronizing and non-synchronizing examples, and the underlying graphs are all connected and non-isomorphic.

To generate a single n -node graph, we use an instance of the Newman-Watts-Strogatz (NWS) model³⁶, which has three parameters n (number of nodes), p (shortcut edge probability), and M (number of calls for adding shortcut edges). Namely, we start from a ring of n nodes, where each node in a cycle is connected to its two nearest neighbors. Then we repeat the following process of adding short edges M times; for each node v , choose a non-adjacent node u , and add an edge between v and u independently with probability p . It is easy to see that each call adds Binomial(n, p) amount of shortcut edges, so the expectation and variance of the number of edges is $n(1 + Mp)$ and $Mnp(1 - p)$, respectively.

Dynamics	Features	Label
$(X_t)_{0 \leq t \leq r}$	See caption	$\mathbf{1}(X_T \text{ is concentrated}^*)$

TABLE II. Structure of each data point in the dynamics data set. We use the following six features: number of edges, min degree, max degree, diameter, number of nodes, and quartiles of initial phases in X_0 . See (6) for the definition of phase-concentration.

Datasets	KM ₁₅	KM ₃₀	FCA ₁₅	FCA ₃₀	GHM ₁₅	GHM ₃₀
# nodes	15	30	15	30	15	30
avg of # edges	29.65	57.49	23.91	47.45	22.88	48.18
std of # edges	3.42	5.67	2.34	4.15	2.35	4.11
r (training iter)	126	126	25	25	25	25
T (prediction iter)	1758	1758	70	70	70	70
# Sync.	100K	40K	100K	40K	100K	40K
# Nonsync.	100K	40K	100K	40K	100K	40K
Features	✓	✓	✓	✓	✓	✓
File size (\approx)	2.2GB	5.3GB	2.1GB	5.2GB	2.1GB	5.2GB

TABLE III. Dynamics datasets generated for three models with two node counts. In each dataset, all graphs are connected and non-isomorphic. # Sync. denotes the number of examples in the dataset such that the phase configuration X_T at iteration T is concentrated (see (6)).

In Table III, we give a summary of the six datasets on the three models for two node counts $n = 15, 30$, each with 200K and 80K examples, respectively, which we refer to as KM_n , FCA_n , GHM_n for $n = 15, 30$. Underlying graphs are sampled from the NWS model with parameters $n \in \{15, 30\}$, $N = 1$, and $p = 0.85$ for KM and $p = 0.65$ for FCA and GHM. In all cases, we generated about 400K examples and subsampled 200K and 80K examples for $n = 15, 30$, respectively, so that there are an equal number of synchronizing and non-synchronizing examples, with all underlying graphs as non-isomorphic. The limits for both sets were chosen by memory constraints imposed by the algorithms used. To give a glance

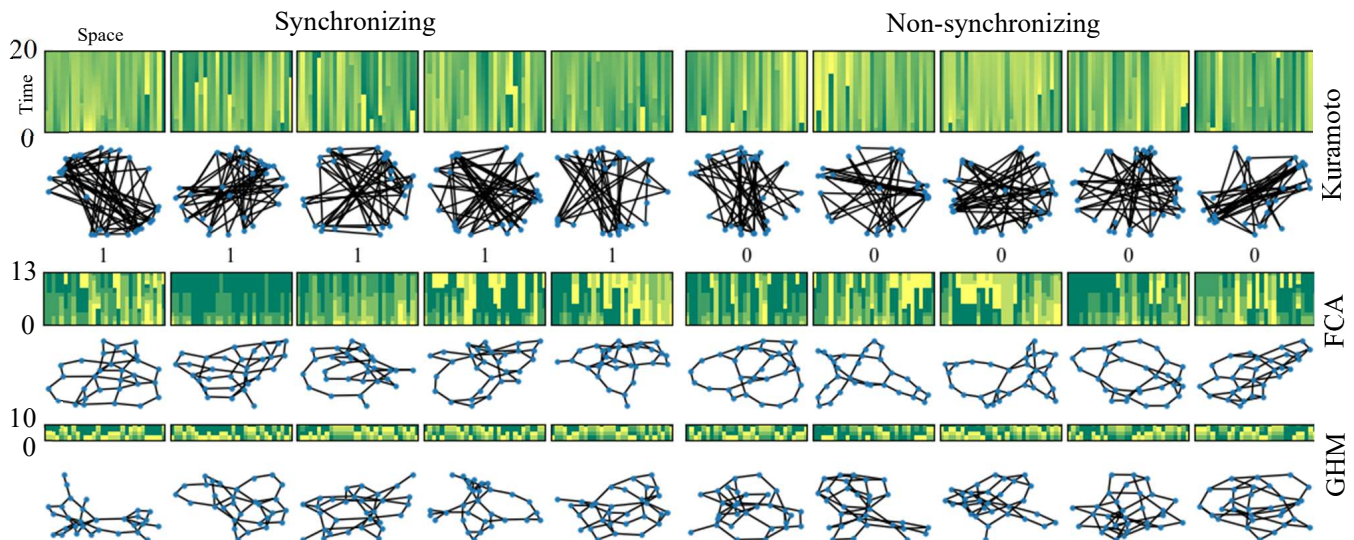


FIG. 4. Sample points in the 30-node training data set for synchronization prediction. The full dataset consists of 40K synchronizing and 40K non-synchronizing 30-node connected non-isomorphic graphs and dynamics on them for each of the three models KM, FCA, and GHM (Table III). Together with features listed in the caption of Table IV, dynamics up to the first r iterations are used for training. For instance, when $r = 20, 13,$ and 4 for KM, FCA, and GHM, respectively, our best method (LRCN) achieves prediction accuracy of 73% (baseline 55%), 84% (baseline 52%), and 96% (baseline 50%) for KM, FCA, and GHM, respectively. See Figure 6. See the caption of Figure 1 for description of the heat maps.

Datasets	FCA ₆₀₀	FCA' ₆₀₀	FCA'' ₆₀₀
# nodes	600	600	300-600
avg of # edges	2985.53	4749.24	2799.49
std of # edges	37.85	2371.72	1461.08
r (training iterations)	25	25	25
T (prediction iterations)	600	600	600
# Sync.	32K	32K	32K
# Nonsync.	32K	32K	32K
Features	✓	✓	✓
File size (\approx)	1.71GB	1.29GB	1.71GB

TABLE IV. Dynamics datasets generated for FCA on 600 nodes (FCA₆₀₀ and FCA'₆₀₀) and on 300-600 nodes (FCA''₆₀₀). In each dataset, all graphs are connected and non-isomorphic. # Sync. denotes the number of examples in the dataset such that the phase configuration X_T at iteration T is concentrated (see (6)).

of the datasets, we provide visual representations. In Figure 4, we show five synchronizing and non-synchronizing examples in KM₃₀, FCA₃₀, and GHM₃₀ (see (6)).

We also generated three dynamics datasets with a larger number of nodes on FCA dynamics, as described in Table IV. The first two datasets FCA₆₀₀ and FCA'₆₀₀ each consists of 32K synchronizing and non-synchronizing examples of FCA dynamics on non-isomorphic graphs of 600 nodes. The underlying graphs are generated by the NWS model with parameters $n = 600, p = 0.6$ and $N = 5$ for FCA₆₀₀; and $p \sim \text{Uniform}(0,1)$ for each $N \sim \text{Uniform}(\{1, 2, \dots, 20\})$ calls on FCA'₆₀₀. Consequently, the number of edges in the graphs from FCA₆₀₀ are sharply concentrated around its mean whereas FCA'₆₀₀ has much greater overall variance in the number of edges (see Table IV). For the last dataset, FCA''₆₀₀, we kept $p \sim \text{Uniform}(0,1)$

for each $N \sim \text{Uniform}(\{1, 2, \dots, 20\})$ calls of adding shortcut edges, but additionally varied the number of nodes as $n \sim \text{Uniform}(\{300, 301, \dots, 600\})$. In this case, both the number of nodes and edges have relatively greater variation compared to FCA₆₀₀.

C. Machine learning algorithms for binary classification

Different machine learning algorithms were employed to solve the problem of predicting whether or not a given graph and initial coloring for a system of coupled oscillators will tend to a synchronizing or non-synchronizing trajectory.

Random Forest (RF)⁴: A random forest is a form of ensemble learning that produces decision trees, and in which these trees themselves are generated using random feature vectors that are sampled independently from a distribution.

Our implementation imposes a limit on the maximum amount of features used per tree to be the square root of the total amount of features in our dataset, \sqrt{p} (where p is the number of features), and uses 100 estimator trees with iterates terminating at complete node purity.

Gradient Boosting (GB)¹⁵: Gradient boosting (GB) is an ensemble learning algorithm for classification tasks similar to RFs where a loss function is minimized by a collection of decision trees to form a strong learner from a group of weak learners. The main difference is that the trees are not trained simultaneously, as in RFs, but added iteratively, so that the current loss is reduced cumulatively so in each iteration for each tree.

Our implementation uses a learning rate of 0.4, 100 estimator trees, and the square root of total number of features per tree when searching for splits.

Feed-forward Neural Networks (FFNN)³: Feedforward Neural Networks (FFNN) form a class of function approximators consisting of multiple layers of connected linear and non-linear activation functions^{6,21}. The linear maps are parameterized by ‘weights’, which are subject to training on a given dataset. The algorithm works by iterating two phases. The first phase is the ‘feed-forward’ phase; the input is mapped to an output by applying the layers of linear and non-linear activation functions with the current weights. The loss between the output and the target labels are then computed. The second phase is the ‘back-propagation’ phase; the weights are modified in the direction that reduces the computed loss from the forward propagation phase.

Our implementation of an FFNN uses a learning rate of 0.01, cross-entropy loss, 4 fully connected linear layers, a hidden layer size of 100, ReLU activation, batch normalization, batch size 256, and dropout of 0.25 probability across 35 epochs. See⁴³ for backgrounds and jargons.

Graph LRCN: A Long-term Recurrent Convolutional Network (LRCN)⁸ is a neural network architecture that has been developed for video data classification by combining convolutional neural networks²⁴ and a special type of recurrent neural network known as the Long Short-Term Memory network (LSTM-Net)²⁰. We propose a variant of LRCN that is suitable for learning to predict dynamics on graphs, which we call the *GraphLRCN*. The idea is to encode each configuration X_t on a graph G as a weighted adjacency matrix $\Delta(X_t)$ of G . Then the dynamics $(X_t)_{0 \leq t \leq r}$ can be turned into a sequence of square matrices, which can be viewed as video data subject to classification. See Figure 5 for an illustration of GraphLRCN.

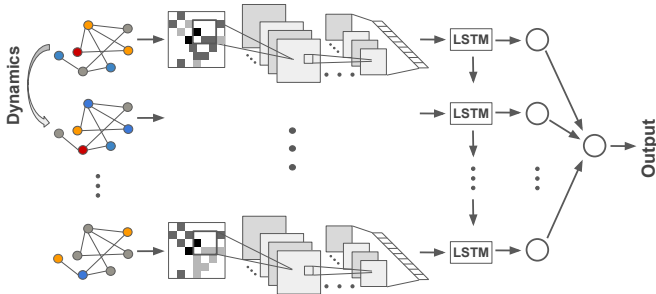


FIG. 5. Architecture of Graph Long-term Recurrent Convolutional Network (LRCN) for synchronization prediction. Dynamics $(X_t)_{0 \leq t \leq r}$ on a graph G are encoded as a sequence of color difference matrices $(\Delta(X_t))_{0 \leq t \leq r}$ and gets fed into the LRCN layers.

Here we give a precise definition of the encoding $X_t \mapsto \Delta(X_t)$. Given a κ -coloring X on a graph $G = (V, E)$, we define the associated *color displacement matrix* $\Delta = \Delta(X) \in (\mathbb{Z}_\kappa)^{|V| \times |V|}$ as

$$\Delta(i, j) = \min \begin{pmatrix} X(i) - X(j) \pmod{\kappa} \\ X(j) - X(i) \pmod{\kappa} \end{pmatrix} \mathbf{1}((i, j) \in E). \quad (7)$$

If $X : V \rightarrow [0, 2\pi)$ is a configuration for KM, we define the associated color displacement matrix $\Delta(X)$ similarly as above by replacing $\text{mod } \kappa$ with $\text{mod } 2\pi$. One can think of $\Delta(X)$ as the adjacency matrix of G weighted by the color differences assigned by X on the edges. An important feature of this encoding is that $\Delta(X)(i, j)$ is nonzero if and only if nodes i, j are adjacent in G and have different colors $X(i) \neq X(j)$. For instance, if X is synchronized then $\Delta(X)$ is the zero matrix. Additionally, since the convolutional block components learn physical location-based associations in the matrix, we applied the reverse Cuthill-Mckee algorithm⁷ on the sequences of adjacency matrices to reduce our matrix bandwidths and augment these physical associations in our representations. In combination, the techniques mentioned are intended to reduce the amount of unnecessary information and noise in the encoding for the purpose of learning to predict synchronization.

D. Scaling up by learning from subsamples

In this subsection, we discuss a way to extend our method for the dynamics prediction problem simultaneously in two directions; 1) larger graphs and 2) variable number of nodes. The idea is to train our dynamics predictor on subsampled dynamics of large graphs (specified as induced subgraphs and induced dynamics), and to combine the local classifiers to make a global prediction. In the algorithm below, $f(X_T) := \mathbf{1}(X_T \text{ is concentrated})$, and if X_t is a phase configuration on $G = (V, E)$ and $G_i = (V_i, E_i)$ is a subgraph of G , then $X_t|_{G_i}$ denotes the restriction $v \mapsto X_t(v)$ for all $v \in V_i$.

Algorithm 1 Ensemble Prediction of Synchronization

- 1: **Input:** Dynamics dataset on graphs with $\geq N$ nodes; Test point $(G', (X'_t)_{0 \leq t \leq r})$;
 - 2: **Parameters:** $n_0 \leq N$ (size of subgraphs), $k_{\text{train}}, k_{\text{test}}$ (# of subgraphs), θ (prediction threshold)
 - 3: **Subsample Dynamics:**
 - 4: For each data point $(G, (X_t)_{0 \leq t \leq r}, f(X_T))$:
 - 5: Sample n_0 -node connected subgraphs $G_1, \dots, G_{k_{\text{train}}}$ of G ;
 - 6: Form restricted triples $(G_i, (X_t|_{G_i})_{0 \leq t \leq r}, f(X_T))$
 - 7: **Train Dynamics Predictor:**
 - 8: Train a binary classifier on the restricted triples;
 - 9: **Ensemble Prediction:**
 - 10: Sample n_0 -node connected subgraphs $G'_1, \dots, G'_{k_{\text{test}}}$ of G' ;
 - 11: $\hat{f} :=$ mean of predictions of $f(X_T)$ on subdynamics on G'_i 's
 - 12: **Output:** $\mathbf{1}(\hat{f} > \theta)$
-

IV. RESULTS

A. Synchronization prediction accuracy for 15-30 node graphs

We apply the four binary classification algorithms for the six datasets described in Table III in order to learn to predict synchronization. Tables III and II provide basic statistics and characterizations of graph structure from these datasets. Figure 7 shows the empirical distribution of the first instance (in

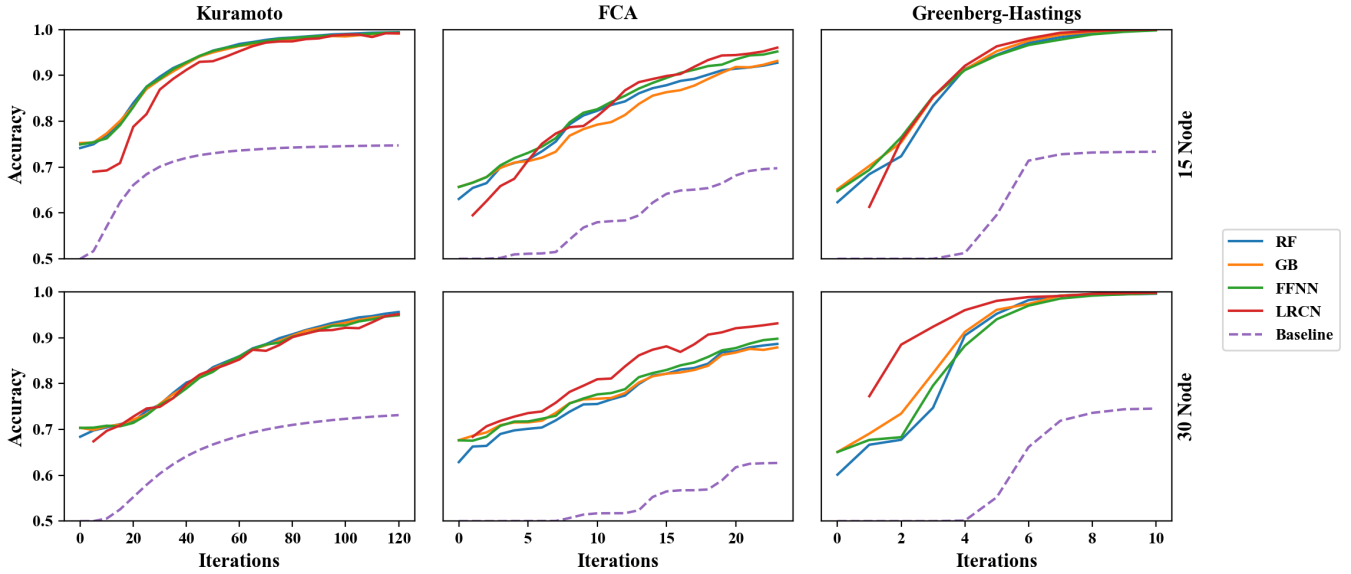


FIG. 6. Synchronization prediction accuracy of four machine learning algorithms for the KM, FCA and GHM coupled oscillators synchronization. For each of the six datasets in Table III, we used 5-fold cross-validation with 80/20 split of test/train. Accuracy is measured by the ratio of the number of correctly classified examples to the total number of examples.

iterations) to reach concentrated among all synchronizing examples in datasets KM_{30} , FCA_{30} and GHM_{30} .

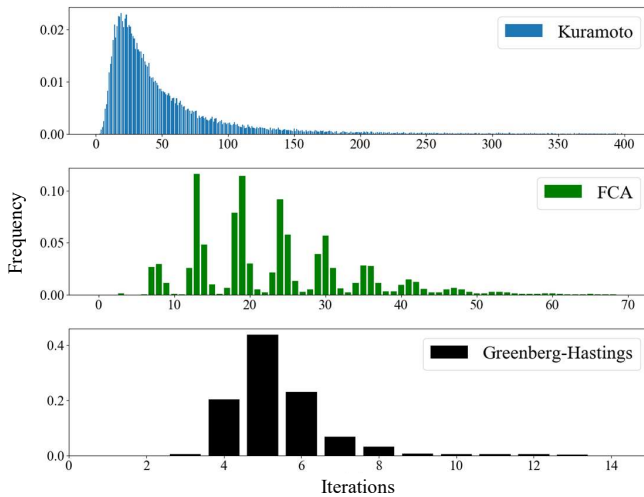


FIG. 7. Empirical distributions on the number of iterations at which synchronizing examples in the dynamics datasets KM_{30} (top), and FCA_{30} (middle), GHM_{30} (bottom) become phase-concentrated.

In Figure 6, we report the synchronization prediction accuracy for six 15-30 node datasets described in Table III. For each dataset, we plot prediction accuracy using four classification algorithms (RF, GB, FFNN, LRCN) and the baseline predictor versus the amount of iterations r used for training. We also use the features listed in the caption of Table III for training.

First, from the classification accuracy at iteration 0, in Figure 6, we see that in using all six features listed in the caption of Table IV, the FFNN, GB and RF binary classification meth-

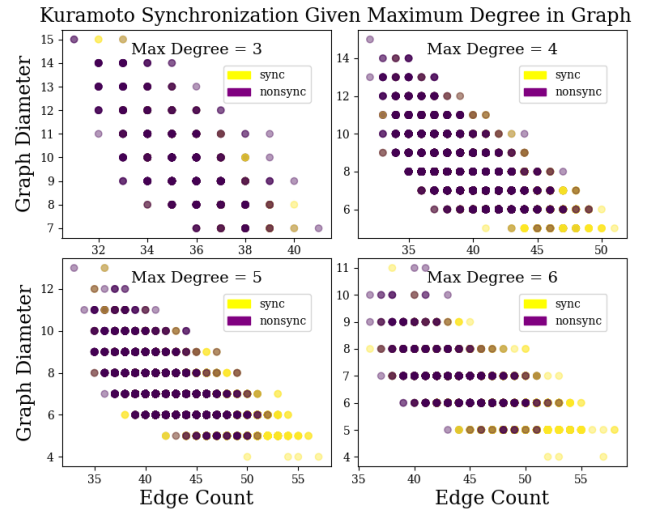


FIG. 8. Multi-dimensional scaling plot of KM_{30} with respect to three features of number of edges, diameter, and maximum degree of underlying graphs. Sample points that synchronize or not during the first 1758 iterations appear as yellow and purple dots, respectively.

ods achieve a classification accuracy approximately 70%. The GraphLRCN binary classifier is offset with respect to the other algorithms as it is fed dynamics information for the adjacency matrix encoding described in (7). To see how each feature contributes to this classification accuracy in more detail, we show a multi-dimensional scaling plot of KM_{30} with respect to the number of edges, diameter, and maximum degree of underlying graphs in Figure 8. From this, it appears that there are more synchronizing examples in KM_{30} than non-synchronizing ones when the maximum degree is at least t , the graph diameter is at most 7, and the number of edges is at least 50.

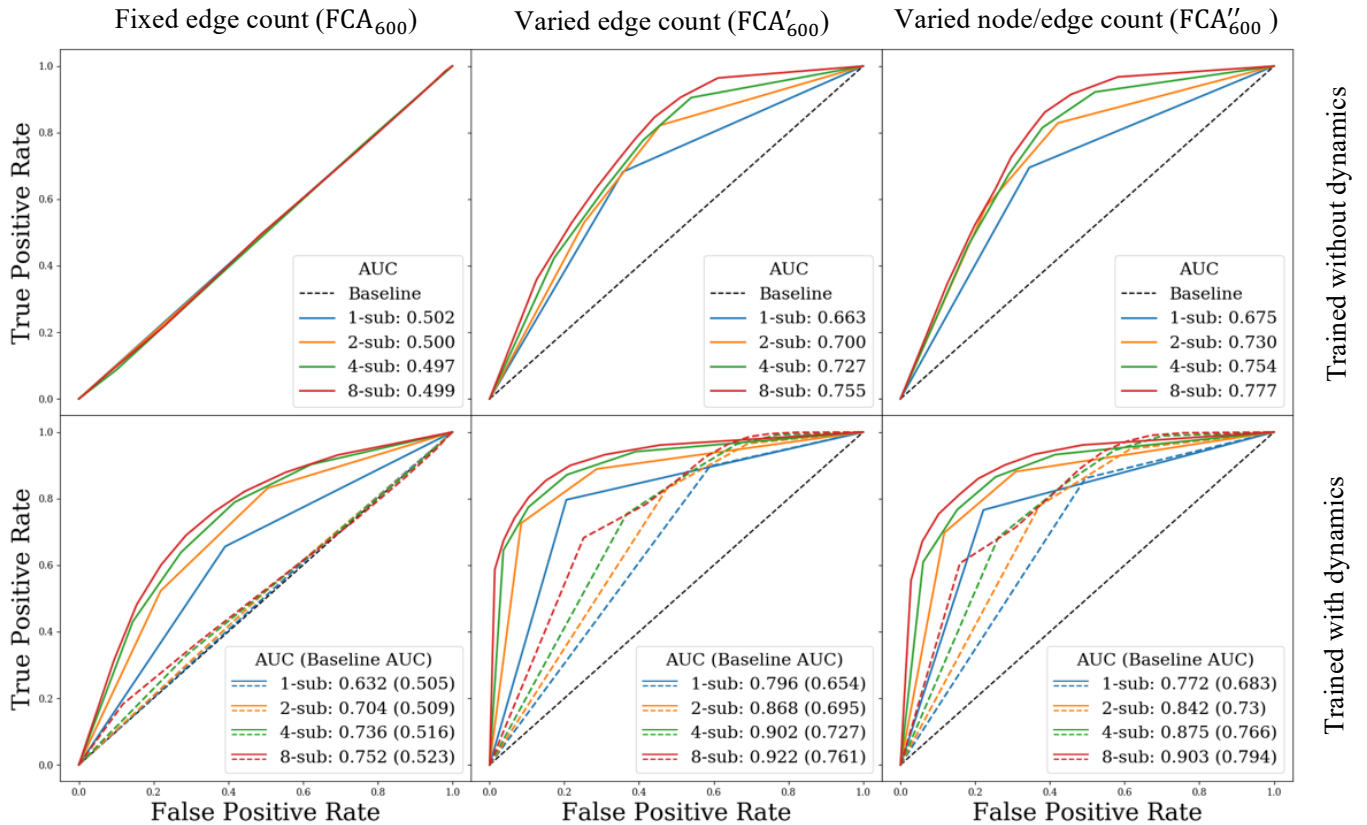


FIG. 9. Receiver-operating-characteristic (ROC) curves for predicting synchronization of 5-color FCA on 600-node graphs from dynamics observed from $k \in \{1, 2, 4, 8\}$ subgraphs of 30 nodes. The ROC curves in the second row are obtained by training with dynamics up to 25 iterations. Corresponding ROC curves using the baseline predictor are shown as dashed lines (with the same color). The area-under-curve (AUC) scores for using k subgraphs are given by ‘ k -sub: AUC (Baseline AUC)’.

Second, we find that as we train the binary classifiers on additional dynamics information, the classification accuracy improves for all cases and for all classifiers; additionally, all four classifiers significantly outperform the baselines in all cases. The classifiers show similar performance for KM and FCA, and the GraphLRCN classifier consistently outperforms the other models, especially so with GHM on 30 nodes. For instance, when $r = 20, 10$ and 4 for KM_{30} , FCA_{30} and GHM_{30} , respectively, our best method (GraphLRCN) achieves a prediction accuracy of 73% (baseline 55%, 1.25% concentrates), 84% (baseline 52%, 1% concentrates) and 96% (baseline 50%, 0% concentrates), respectively.

Third, it appears that the Kuramoto model is harder to predict synchronization compared to the two discrete models with just static graph information, and GHM appears to be the easiest to predict synchronization in general. For instance, for GHM on both node counts, training all four classifiers on $r = 4$ iterations produces a prediction accuracy of at least 90%, while the baseline achieves only 50%.

B. Synchronization prediction accuracy for 300-600 node graphs

We apply the ensemble prediction method (Algorithm 1) to the three dynamics datasets for the FCA described in Table

IV. In Figures 9, we report the synchronization prediction accuracy of the ensemble predictor (Algorithm 1) on the datasets FCA_{600} , FCA'_{600} , FCA''_{600} described in Table IV. We used Algorithm 1 with $n_0 = 30$ (size of subgraphs), $k \in \{1, 2, 4, 8\}$ (# of subgraphs). The binary classification algorithm we used is the FFNN. As a baseline, we can apply algorithm 1 with the baseline predictor in Subsection III A as the choice of binary classifier. The prediction threshold θ is varied from 0 to 1, and the result is represented as a receiver operating characteristic (ROC) together with the area-under-curve (AUC) metric for prediction accuracy. $AUC = 1$ means perfect prediction. The first two columns of Figures 9 show results for FCA_{600} and FCA'_{600} , and the first and second rows of the figure corresponds to $r = 0$ (trained only on the features of subgraphs and initial configuration) and $r = 25$ (trained with $r = 25$ iterations of induced dynamics on subgraphs). Note that since our datasets have an equal number of synchronizing and non-synchronizing examples, the baseline AUC for $r = 0$ is 0.5 regardless of the number k of sampled subgraphs.

First, for FCA_{600} where the graphs have the same number of nodes and a similar number of edges (see Table IV), we hardly gain any prediction accuracy when trained without dynamics. But training with $r = 25$ iterations with $k \geq 2$ subgraphs improves the AUC by 0.20, where the baseline AUC stays close

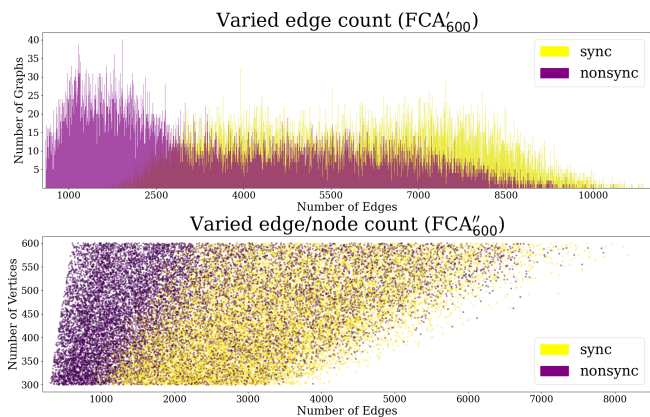


FIG. 10. (Top) Histogram for edge counts of data points in FCA'_{600} . (Bottom) Scatterplot of data points in FCA''_{600} with respect to node and edge counts.

to 0.500. Note that from the iteration-until-concentration histogram in Figure 11, we see that there are almost no synchronizing examples in FCA_{600} that synchronize in the first $r = 25$ iterations, which explains baseline AUC being close to even in this case.

Second, we observe that both the ensemble predictor and the baseline perform better (AUC greater by at least 0.16 in all cases) for datasets consisting of graphs with a diverse number of edges (FCA'_{600} and FCA''_{600}) than for FCA_{600} . For instance, using only $k = 2$ subgraphs of 30 nodes, we achieve AUC scores of 0.868 (baseline 0.695) for FCA'_{600} and 0.842 (baseline 0.730) for FCA''_{600} . The gain in accuracy for training without dynamics indicates that having more diverse edge (and or node) counts in the dataset could make it easier to predict synchronization by only using the initial features. Indeed, from the top histogram of FCA'_{600} in Figure 10, we see that there are significantly more non-synchronizing examples of smaller edge count of FCA'_{600} , which explains the jump in the prediction accuracy from FCA_{600} to FCA'_{600} even with training without dynamics. Moreover, the scatterplot of data points in FCA''_{600} with respect to node and edge count at the bottom of Figure 10 shows that there are significantly more non-synchronizing examples in FCA''_{600} with smaller edge count regardless of node count. On the other hand, the gain in accuracy for training with dynamics can be seen from the iteration-to-synchronization histogram in Figure 11; there, we see that about 15-30% of synchronizing examples in FCA'_{600} and FCA''_{600} do synchronize by iteration $r = 25$.

C. Discussion

Predicting whether a given system of coupled oscillators with an underlying arbitrary graph structure will synchronize is an important yet analytically intractable problem. In this work, we proposed an alternative approach to this problem by viewing it as a binary classification task, where each data point consisting of a graph paired with the corresponding initial dynamics for a given model needs to be classified into two

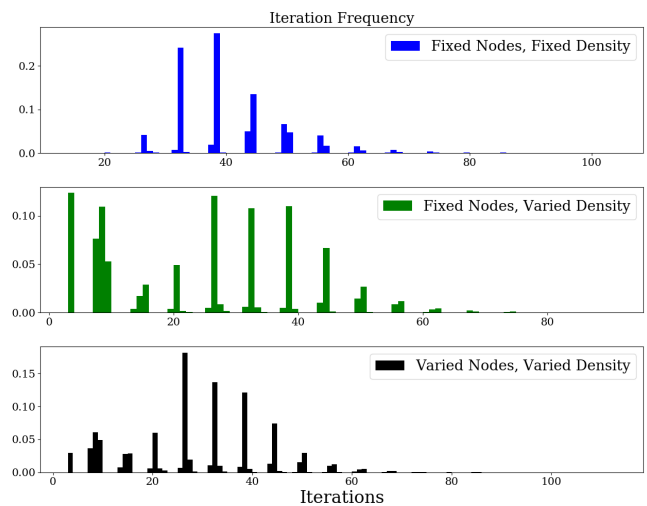


FIG. 11. Empirical distribution of iterations until concentration for the synchronizing examples in datasets FCA_{600} (top), FCA'_{600} (middle), and FCA''_{600} (bottom).

classes of ‘synchronizing’ and ‘non-synchronizing’ dynamics. We have shown that, once trained on large enough datasets of synchronizing and non-synchronizing dynamics on heterogeneous graphs, a number of binary classification machine learning algorithms can indeed successfully predict the synchronization of unknown systems with accuracy far exceeding a baseline utilizing the well-known ‘concentration principle’ in dynamical systems. Furthermore, we have also proposed the ‘ensemble predictor’ that scales up our method to larger graphs by applying our method on randomly sampled and relatively small collections of induced subgraphs and aggregating the local prediction results. This method was able to outperform the baseline prediction method by learning latent cues of synchronizing and non-synchronizing examples from both initial features and dynamic information. With these results, we believe that our work is able to provide a new insight to similar problems in complex dynamical systems.

Given that our machine learning approach is able to achieve high prediction accuracy, we suspect that there may be some analytically tractable characterizations on graphs paired with corresponding initial dynamics signaling eventual synchronization or not, which we are yet to establish rigorously. As mentioned at the end of Subsection IC, previously known of such characterizing conditions include the initial vector field on the edges induced by the initial color differential for the 3-color GHM and CCA¹⁶, as well as the number of available states being strictly less than the maximum degree of underlying trees for the FCA^{27,28}. Designing similar target features into datasets and training binary classification algorithms could guide further analytic discovery of such conditions for the coupled oscillator models considered in this work.

Furthermore, even though we have focused on predicting only two classes of long-term behavior of complex dynamical systems as only synchronizing and non-synchronizing dynamics, our method can readily be extended to predicting an arbitrary

trary number of classes of long-term behaviors. For instance, one can consider the κ -state voter model on graphs, where the interest would be the final dominating color. In such circumstances, one can train κ -state classification machine learning algorithms on datasets of heterogeneous graphs. Beyond κ -state classification our method can be extended to predicting a continuous variable that is associated to a complex dynamical systems on graphs. For instance, if each node in a graph represents a particular stock in a financial model, could one predict the long-term value of a portfolio given by the ensemble of such stocks that interact with each other? For such problems, one could train a regression model on datasets generated on heterogeneous graphs to gain insights on how the limiting aggregate value of the entire system of interacting assets is influenced by the underlying graph structure.

Finally, a more ambitious task beyond long-term dynamic behavior quantified by a single metric is the potential extension of our methods to full time-series and graph state regression. In other words, if each node in the graph represents an individual in an arbitrary social network, can we predict the sentiment level for a given topic at any given time t for every single individual in that particular social network? One can again generate large overarching social networks and run many simulations of sentiment dynamics with many possible edge configurations between individuals (for example, measured by the number of mutual friends or likes/shares of posts on social media). The ultimate goal would be a framework for learning to predict, with precision, entire trajectories of complex dynamical systems.

ACKNOWLEDGMENTS

This work is supported by NSF grant [DMS-2010035](#). We are also grateful for partial supports from and the Department of Mathematics and the Physical Sciences Division at UCLA. We also thank Andrea Bertozzi and Deanna Needell for supports and helpful discussions. JV is partially supported by Deanna Needell's grant NSF BIGDATA DMS #1740325.

REFERENCES

- ¹Juan A Acebrón, Luis L Bonilla, Conrad J Pérez Vicente, Félix Ritort, and Renato Spigler. The kuramoto model: A simple paradigm for synchronization phenomena. *Reviews of modern physics*, 77(1):137, 2005.
- ²Umberto Biccari and Enrique Zuazua. A stochastic approach to the synchronization of coupled oscillators. 2020.
- ³Christopher M Bishop. *Pattern recognition and machine learning*. springer, 2006.
- ⁴Leo Breiman. Random forests. *Machine learning*, 45(1):5–32, 2001.
- ⁵Bernard Chazelle. The total s-energy of a multiagent system. *SIAM Journal on Control and Optimization*, 49(4):1680–1706, 2011.
- ⁶Balázs Csanád Csáji et al. Approximation with artificial neural networks. *Faculty of Sciences, Eötvös Loránd University, Hungary*, 24(48):7, 2001.
- ⁷Elizabeth Cuthill and James McKee. Reducing the bandwidth of sparse symmetric matrices. In *Proceedings of the 1969 24th national conference*, pages 157–172, 1969.
- ⁸Jeffrey Donahue, Lisa Anne Hendricks, Sergio Guadarrama, Marcus Rohrbach, Subhashini Venugopalan, Kate Saenko, and Trevor Darrell. Long-term recurrent convolutional networks for visual recognition and description. In *Proceedings of the IEEE conference on computer vision and pattern recognition*, pages 2625–2634, 2015.
- ⁹Florian Dorfler and Francesco Bullo. Synchronization and transient stability in power networks and nonuniform kuramoto oscillators. *SIAM Journal on Control and Optimization*, 50(3):1616–1642, 2012.
- ¹⁰Richard Durrett and Jeffrey E Steif. Some rigorous results for the greenberg-hastings model. *Journal of Theoretical Probability*, 4(4):669–690, 1991.
- ¹¹Robert Fisch. Cyclic cellular automata and related processes. *Physica D: Nonlinear Phenomena*, 45(1):19–25, 1990.
- ¹²Robert Fisch. The one-dimensional cyclic cellular automaton: a system with deterministic dynamics that emulates an interacting particle system with stochastic dynamics. *Journal of Theoretical Probability*, 3(2):311–338, 1990.
- ¹³Robert Fisch. Clustering in the one-dimensional three-color cyclic cellular automaton. *The Annals of Probability*, pages 1528–1548, 1992.
- ¹⁴Robert Fisch, Janko Gravner, and David Griffeath. *Cyclic cellular automata in two dimensions*. Springer, 1991.
- ¹⁵Jerome H Friedman. Stochastic gradient boosting. *Computational statistics & data analysis*, 38(4):367–378, 2002.
- ¹⁶Janko Gravner, Hanbaek Lyu, and David Sivakoff. Limiting behavior of 3-color excitable media on arbitrary graphs. *Annals of Applied Probability (to appear)*, 2016.
- ¹⁷Janko Gravner, Hanbaek Lyu, David Sivakoff, et al. Limiting behavior of 3-color excitable media on arbitrary graphs. *The Annals of Applied Probability*, 28(6):3324–3357, 2018.
- ¹⁸James M Greenberg and SP Hastings. Spatial patterns for discrete models of diffusion in excitable media. *SIAM Journal on Applied Mathematics*, 34(3):515–523, 1978.
- ¹⁹Ahmed Hefny, Carlton Downey, and Geoffrey Gordon. Supervised learning for dynamical system learning. 2015.
- ²⁰Sepp Hochreiter and Jürgen Schmidhuber. Long short-term memory. *Neural computation*, 9(8):1735–1780, 1997.
- ²¹Kurt Hornik. Approximation capabilities of multilayer feedforward networks. *Neural networks*, 4(2):251–257, 1991.
- ²²Kazuha Itabashi, Quoc Hoan Tran, and Yoshihiko Hasegawa. Evaluating the phase dynamics of coupled oscillators via time-variant topological features. 2020.
- ²³Johannes Klinglmayr, Christoph Kirst, Christian Bettstetter, and Marc Timme. Guaranteeing global synchronization in networks with stochastic interactions. *New Journal of Physics*, 14(7):073031, 2012.
- ²⁴Alex Krizhevsky, Ilya Sutskever, and Geoffrey E Hinton. Imagenet classification with deep convolutional neural networks. *Communications of the ACM*, 60(6):84–90, 2017.
- ²⁵Yoshiki Kuramoto. *Chemical oscillations, waves, and turbulence*. Courier Corporation, 2003.
- ²⁶Tony E. Lee, Heywood Tam, G. Refael, Jeffrey L. Rogers, and M. C. Cross. Vortices and the entrainment transition in the two-dimensional kuramoto model. *Physical Review E*, 82(3), Sep 2010.
- ²⁷Hanbaek Lyu. Synchronization of finite-state pulse-coupled oscillators. *Physica D: Nonlinear Phenomena*, 303:28–38, 2015.
- ²⁸Hanbaek Lyu. Phase transition in firefly cellular automata on finite trees. *arXiv preprint arXiv:1610.00837*, 2016.
- ²⁹Hanbaek Lyu. Global synchronization of pulse-coupled oscillators on trees. *To appear in SIAM Journal on Applied Dynamical Systems*. Preprint available at [arXiv:1604.08381](#), 2017.
- ³⁰Hanbaek Lyu and David Sivakoff. Persistence of sums of correlated increments and clustering in cellular automata. *Submitted*. Preprint available at [arXiv.org/1706.08117](#), 2017.
- ³¹Hanbaek Lyu and David Sivakoff. Synchronization of finite-state pulse-coupled oscillators on \mathbb{Z} . [arXiv.org:1701.00319](#), 2017.
- ³²Erik A Martens, Carlo R Laing, and Steven H Strogatz. Solvable model of spiral wave chimeras. *Physical review letters*, 104(4):044101, 2010.
- ³³Brendan McKay. Combinatorial data. <http://users.cecs.anu.edu.au/~bkm/data/graphs.html>, 2020.
- ³⁴Luc Moreau. Stability of multiagent systems with time-dependent communication links. *Automatic Control, IEEE Transactions on*, 50(2):169–182, 2005.

- ³⁵Sujit Nair and Naomi Ehrich Leonard. Stable synchronization of rigid body networks. *Networks and Heterogeneous Media*, 2(4):597, 2007.
- ³⁶Mark EJ Newman, Duncan J Watts, and Steven H Strogatz. Random graph models of social networks. *Proceedings of the National Academy of Sciences*, 99(suppl 1):2566–2572, 2002.
- ³⁷Joel Nishimura and Eric J Friedman. Robust convergence in pulse-coupled oscillators with delays. *Physical review letters*, 106(19):194101, 2011.
- ³⁸Felipe Nunez, Yongqiang Wang, and Francis J Doyle. Synchronization of pulse-coupled oscillators on (strongly) connected graphs. *Automatic Control, IEEE Transactions on*, 60(6):1710–1715, 2015.
- ³⁹Roberto Pagliari and Anna Scaglione. Scalable network synchronization with pulse-coupled oscillators. *IEEE Transactions on Mobile Computing*, 10(3):392–405, 2011.
- ⁴⁰Antonios Papachristodoulou, Ali Jadbabaie, and Ulrich Munz. Effects of delay in multi-agent consensus and oscillator synchronization. *Automatic Control, IEEE Transactions on*, 55(6):1471–1477, 2010.
- ⁴¹Anton V Proskurnikov and Ming Cao. Synchronization of pulse-coupled oscillators and clocks under minimal connectivity assumptions. *arXiv preprint arXiv:1510.02338*, 2015.
- ⁴²Steven H Strogatz. From kuramoto to crawford: exploring the onset of synchronization in populations of coupled oscillators. *Physica D: Nonlinear Phenomena*, 143(1):1–20, 2000.
- ⁴³Daniel Svozil, Vladimir Kvasnicka, and Jiri Pospichal. Introduction to multi-layer feed-forward neural networks. *Chemometrics and intelligent laboratory systems*, 39(1):43–62, 1997.
- ⁴⁴Thomas N. Thiem, Mahdi Kooshkbaghi, Tom Bertalan, Carlo R. Laing, and Ioannis G. Kevrekidis. Emergent spaces for coupled oscillators. *Frontiers in Computational Neuroscience*, 14:36, 2020.